ORGANOMETALLICS

Article

Cite This: *Organometallics* 2018, 37, 3936−3942

pubs.acs.org/Organometallics

# Oxidation of Methylalumoxane Oligomers: A Theoretical Study Guided by Mass Spectrometry

Erik Endres,[†,‡] Harmen S. Zijlstra,[§] Scott Collins,[§] J. Scott McIndoe,[§] and Mikko Linnolahti*[,†]

[†]Department of Chemistry, University of Eastern Finland, P.O. Box 111, FI-80101 Joensuu, Finland

[‡]Faculty of Chemistry & Pharmacy, Julius-Maximilians University, P.O. Box 97074, Würzburg 97070, Germany

[§]Department of Chemistry, University of Victoria, P.O. Box 3065, Victoria, British Columbia V8W 3 V6, Canada

Supporting Information

**ABSTRACT:** Methylalumoxane (MAO) plays a critical role in catalytic polymerization of olefins, both as activator of the precatalyst and scavenger of impurities. The latter involves oxidation of MAO, which is not well understood at a molecular level. On the basis of our previous computational explorations of the structure of MAO and electrospray ionization mass spectrometry (ESI-MS) studies of its oxidation, we report here a systematic theoretical study to shed light on the oxidation process. We identify the structural features of the MAO that are essential for oxidation by screening the thermodynamics of the oxidation reactions as a function of shape and size of the previously justified model MAOs. In correlation with previously reported ESI-MS studies of the corresponding anions (*Chem. Eur. J.* **2018**, *24*, 5506−5512, DOI: 10.1002/chem.201705458), the calculations indicate that Al sites of high Lewis acidity could be of major relevance in the oxidation process. Such sites are abundant in the size domain observed relevant for the corresponding anions.

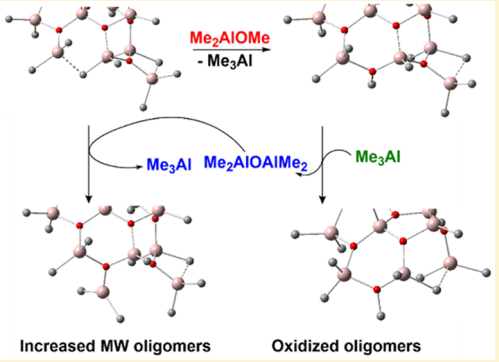


## INTRODUCTION

Polyolefins have gained an irreplaceable status within our daily lives, thanks to complex and highly efficient catalysts systems. One of the growing techniques for preparation of polyolefins is the group IV metallocene/methylalumoxane (MAO) catalyst system, where MAO alkylates and ionizes the metallocene precursors, resulting in a highly active catalyst.[1] However, even though MAO has been used as catalyst activator for decades, its complete structure as well as the exact mechanism of activation remain incompletely defined.[2] Molecular weight depends on the measurements,[3−10] typically ranging from 1000 to 2000 Da, with an average composition of $(Me_{1.4-1.5}AlO_{0.75-0.8})_n$.[11] Various spectroscopic investigations and quantum mechanical calculations indicate that the general molecular formula is best written as $(MeAlO)_x(Me_3Al)_y$, where $x$ is the degree of oligomerization the MAO cluster achieves during its synthesis via hydrolysis of trimethylaluminum (TMA), and $y$ is the number of TMA monomers which are incorporated into the clusters, either as $Me_2AlO_n$ groups ($n$ = 1,2) or as datively bound $Me_3Al$.[12−14]

Recent calculations suggest that the clusters change their shape as a function of $x$ from chains ($x$ = 1−2) to rings ($x$ = 3−4), sheets ($x$ = 5−12), and cages ($x$ = 13−18), and the clusters incorporate up to six monomers of TMA ($y \leq 6$).[15,16] Nearly independent of shape and size, the clusters share a preference for four-coordinate Al, three-coordinate O and terminal as well as pentavalent methyl groups bridging between adjacent Al atoms. The bridge sites, which are discussed in more detail below, are likely the active sites of the MAO activator. The reported calculations[16] find a minimum in Gibbs energy at $x$ = 16, $y$ = 6, in short **16,6**, which following methide abstraction (or indistinguishably $Me_2Al^+$ cleavage from **16,7**, which the calculations find higher in energy) corresponds to the probable composition of the major anion $[(MeAl-O)_{16}(Me_3Al)_6Me]^-$ found recently by electrospray ionization mass spectrometry (ESI-MS) with molecular weight of 1375 Da.[10,13]

Oxidation of MAO plays an important role in the catalytic process. Besides activating the precatalyst, MAO also scavenges impurities like water and oxygen,[17] which are reactive toward the transition metal−carbon bond and hence poison the catalyst. The poisons are present at low levels in the solvent or monomer even after purification in the industrial process. MAO readily reacts with water to further oligomerize to larger clusters and is oxidized by oxygen, eventually leading to aging of MAO. Thus, the concentration of the impurities is lowered to such a degree that the activity of the catalyst remains intact. Little is known about the oxidation mechanism of MAO. However, since MAO contains free TMA, it is reasonable to assume that the first step is the direct oxidation of TMA into $Me_2AlOMe$. While its Ga analogue forms a stable peroxide $Me_2GaOOMe$,[18] the detailed mechanism of oxidation of TMA is not known, though it has been suggested that the dimer of TMA is directly oxidized to form two equivalents of $Me_2AlOMe$.[19]

**Received:** August 16, 2018
**Published:** October 26, 2018






DOI: 10.1021/acs.organomet.8b00587
*Organometallics* 2018, 37, 3936−3942

Recent ESI-MS studies investigated the oxidation process of MAO and proposed a mechanism (Scheme 1),[20] in which

**Scheme 1. Proposed Oxidation Mechanism of MAO[20]**

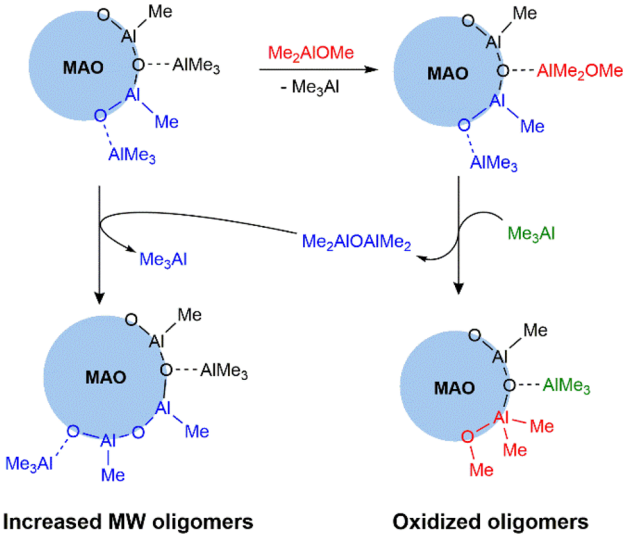


TMA is substituted by $Me_2AlOMe$, the direct oxidation product of TMA. Here we extend these studies by a systematic computational study as a function of size and sites of MAO. Finally, we study a possible route for the rearrangement reaction accompanying the substitution.

## RESULTS AND DISCUSSION

We base our investigations on the most stable MAO structures located for each degree of oligomerization up to $x$ = 18 in previous works (Figure 1).[12,15,16] However, the set is modified to replace **3,3**, **7,4**, and **9,5** by **3,4**, **7,5**, and **9,6**, respectively, which we have newly found to be more stable oligomers at the employed level of theory when the Gibbs energies are corrected for solvation entropy. The relative stabilities of the MAOs are given in Table 1. As has been discussed before, the stabilities peak at **16,6**, which is in qualitative agreement with ESI-MS studies of the corresponding anions.[10,16]

While the MAOs differ in the base structure, varying from chains to rings, sheets, and cages as a function of degree of oligomerization, they possess similar structural features due to incorporation of TMA into the $(MeAlO)_x$ core. These are the sites of interest for consideration of the reactions the MAOs may undergo, and are likely responsible for the cocatalytic activity of MAO. The five frequently occurring sites are illustrated in Figure 2 alongside with the number of total occurrences in the data set shown in Figure 1. Site **E** is Lewis acidic, while sites **A** and **B** possess latent Lewis acidity[21] through opening of the bridging bond during methide abstraction by the MAO from the precatalyst. However, sites **C** and **D** can ionize through $Me_2Al^+$ abstraction from the MAO, which is an alternative route for precatalyst activation. Sites **E** differ from sites **A** or **B**: The latter occur by definition only between germinal Al atoms bonded to the same oxygen atom, while the former occurs between spatially close, but chemically more remote Al atoms. As such, sites **E** may display variable reactivity including the weakest, almost negligible, bridging interactions with a distance of 2.7−3 Å between the methyl and the $Me_2Al$ groups, and hence represent three-coordinate Lewis acidic Al sites under realistic circumstances.

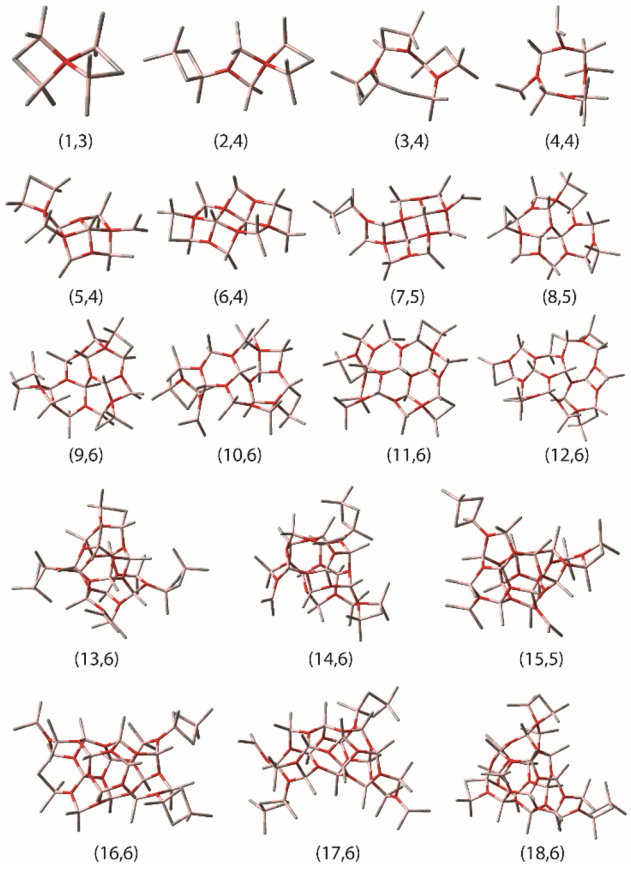


**Figure 1.** Most stable MAOs located for each degree of oligomerization. Hydrogens omitted for clarity; carbon in gray, aluminum in pink, and oxygen in red.

**Table 1. Relative Stabilities of the Studied MAOs**

| $x$ | $y$ | $\Delta(\Delta G/x)^a$ | $\Delta(\Delta G)^b$ | mole fraction[c] |
|---|---|---|---|---|
| 1 | 3 | 11.1 | 11.1 | $1.1 \times 10^{-2}$ |
| 2 | 4 | 10.1 | 20.2 | $2.9 \times 10^{-4}$ |
| 3 | 4 | 12.0 | 36.0 | $4.9 \times 10^{-7}$ |
| 4 | 4 | 7.5 | 30.0 | $5.4 \times 10^{-6}$ |
| 5 | 4 | 4.2 | 21.0 | $2.1 \times 10^{-4}$ |
| 6 | 4 | 4.0 | 24.0 | $6.2 \times 10^{-5}$ |
| 7 | 5 | 6.3 | 44.1 | $1.9 \times 10^{-8}$ |
| 8 | 5 | 4.4 | 35.2 | $6.8 \times 10^{-7}$ |
| 9 | 6 | 4.1 | 36.9 | $3.4 \times 10^{-7}$ |
| 10 | 6 | 6.2 | 62.0 | $1.4 \times 10^{-11}$ |
| 11 | 6 | 3.4 | 37.4 | $2.8 \times 10^{-7}$ |
| 12 | 6 | 2.1 | 25.2 | $3.8 \times 10^{-5}$ |
| 13 | 6 | 2.1 | 27.3 | $1.6 \times 10^{-5}$ |
| 14 | 6 | 1.4 | 19.6 | $3.6 \times 10^{-4}$ |
| 15 | 5 | 1.3 | 19.5 | $3.8 \times 10^{-4}$ |
| 16 | 6 | 0.0 | 0.0 | 0.98 |
| 17 | 6 | 0.7 | 11.9 | $8.1 \times 10^{-3}$ |
| 18 | 6 | 0.9 | 16.2 | $1.4 \times 10^{-3}$ |

[a] $\Delta(\Delta_r G)$ in kJ $mol^{-1}x^{-1}$ for reaction $0.5(x + y)Me_6Al_2 + xH_2O \rightarrow (MeAlO)_x(Me_3Al)_y + 2xCH_4$ at $T$ = 298 K and $p$ = 1 atm with correction to condensed phase by multiplication of the $T\Delta S$ term by 2/3. [b] Difference in free energy of reaction independent of $x$. [c] Determined using the Boltzmann distribution.

We next study the oxidation process taking place on sites **A**−**E** by modeling the cleavage of TMA and subsequent



DOI: 10.1021/acs.organomet.8b00587
Organometallics 2018, 37, 3936−3942

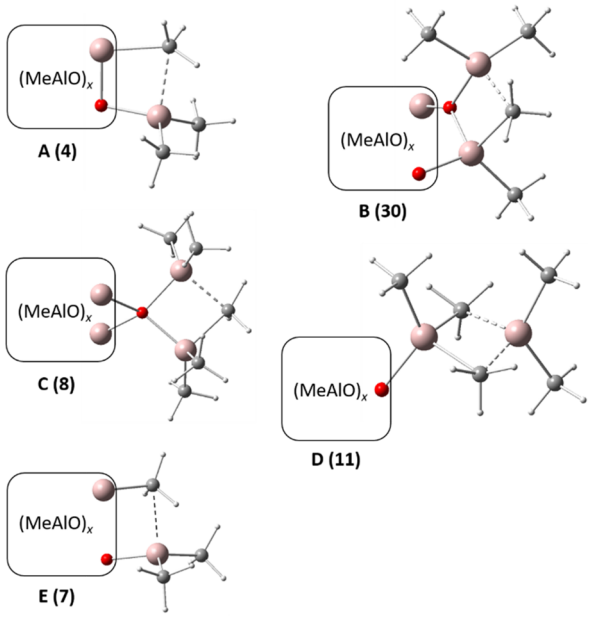


**Figure 2.** Incorporation of TMA into the MAOs. The squares depict the $(MeAlO)_x$ cores, and the numbers in parentheses specify the total number of occurrences in the MAOs shown in Figure 1. Carbon in gray, aluminum in pink, and oxygen in red.

addition of $Me_2AlOMe$ into the whole data set of MAOs. This is the first step invoked in the oxidation of MAO as monitored by ESI-MS.[20] All the results are concisely summarized in Figures 3–5, showing the Gibbs energies of the reactions as a function of size and site, with the latter illustrated by different colors.

Figure 3 shows the Gibbs energies for TMA cleavage, which is endergonic in all cases because the study was carried out for MAOs with the highest relative stability within each degree of oligomerization.[16] Overall, abstraction of TMA from sites of type **D**, followed by sites of type **C**, requires the least amount of energy. Abstraction from both **D** and **C** sites leaves a $Me_2Al$ end group, which can interact with the methyl group of an adjacent Al to form a type **A** site. Sites of type **B** are most common in the data set and are abundant in sheet structures. They show feasible TMA abstraction in the domain of sheet structures ($x$ = 8–12) but not in the domain of cage structures ($x$ = 13–18). Abstraction of TMA from sites of type **A** and **E** leaves an unsaturated oxygen, showing a prohibitively high Gibbs energy with a few exceptions, where the molecule has freedom to reorganize.

Figure 4 shows the Gibbs energies for $Me_2AlOMe$ addition to the MAOs after TMA cleavage. $Me_2AlOMe$ addition is exergonic in each case and for a large degree mirrors the Gibbs energies for TMA cleavage. Addition is thus the most exergonic for sites of type **A** and the least exergonic for sites of type **D**. Replacing Me by bulkier alkyl groups would likely make the reactions less exergonic due to the reduced Lewis acidity of aluminum alkoxides, associated with steric effects.

Figure 5 shows the Gibbs energies for the complete substitution reaction, i.e., the sum of TMA cleavage and $Me_2AlOMe$ substitution. The total reaction is exergonic in almost every case, indicating that the oxidation products are more stable than the corresponding TMA educt. If one would ignore sites **A** and **E** due to the high energy required for TMA cleavage, then the energies are lowest for sites of type **B** in **8,5**, **10,6**, and **11,6**. For cage structures in the real size domain of MAOs with $x$ > 12, the sites most prone to oxidation would then be of type **D**. However, as we later show, sites of type **E**, present in the real size cage structures, could in fact be relevant, especially if direct oxidation of the cages is possible.

We can rationalize the above findings as follows. Since MAOs typically prefer four-coordinate Al and three-coordinate O,[16,22] loss of TMA is by default associated with two-coordinate oxygen at the site of cleavage, thus resulting in the high Gibbs energies seen in many instances in Figure 3. Consequently, sites of the type **D**, where TMA is only connected via bridging methyl groups, are the main candidates for the release of TMA. However, even though three-coordinate oxygens are generally preferred, there are sites generated by associated TMA where oxygen atoms attain four-coordination. Such sites are represented by sites of type **C**, as well as by specific sites of type **B**, which due to the variety of environments lead to largest scattering in the Gibbs energies of TMA cleavage and $Me_2AlOMe$ substitution (red markers in Figures 3–5). Figure 6 illustrates a type **B** site of **10,6** as an example that is low in energy for substitution by $Me_2AlOMe$. A $Me_2Al$--Me moiety, highlighted in purple, is loosely bound to the MAO through formation of a four-coordinate O and $CH_3$ bridging to the adjacent Al. Cleavage of TMA leaves an

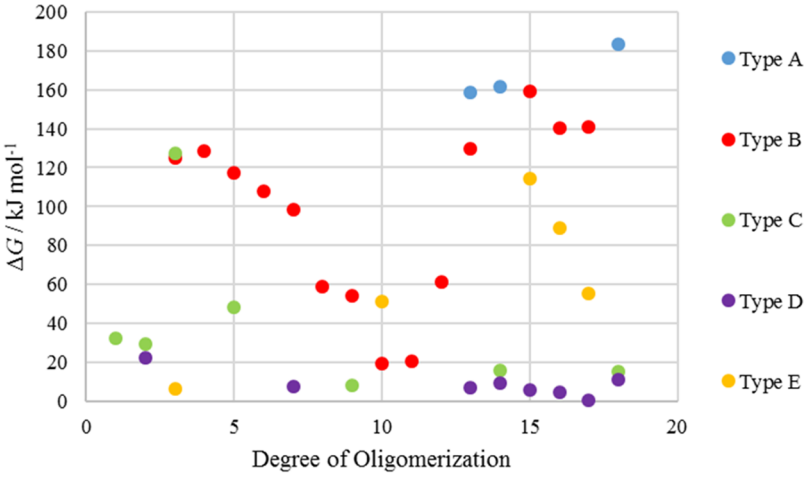


**Figure 3.** Gibbs energies as a function of degree of oligomerization for cleavage of TMA from MAO. The sites **A**–**E** are depicted in Figure 2.



DOI: 10.1021/acs.organomet.8b00587
*Organometallics* 2018, 37, 3936–3942

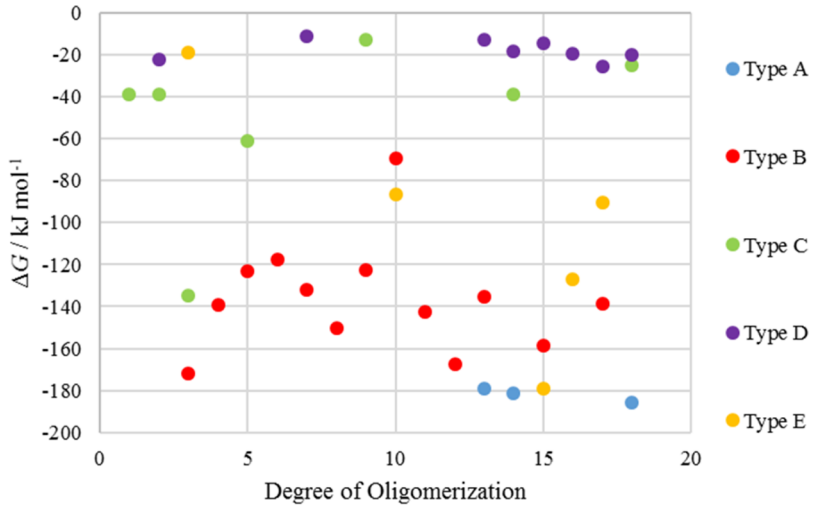


**Figure 4.** Gibbs energies as a function of degree of oligomerization for the addition of $Me_2AlOMe$ after cleavage of TMA. The sites **A**–**E** are depicted in Figure 2.

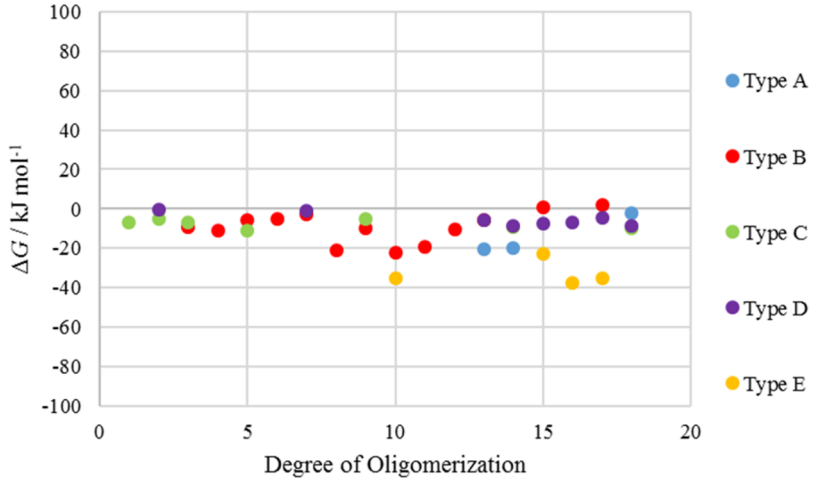


**Figure 5.** Gibbs energies as a function of degree of oligomerization for $Me_3Al$ to $Me_2AlOMe$ substitution. The sites **A**–**E** are depicted in Figure 2.

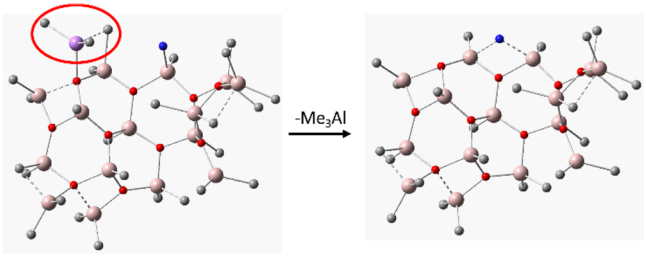


**Figure 6.** Reorganization after TMA cleavage to form a methyl bridge, illustrated for site **B** in **10,6** as an example. The removed Al and the bridging carbon are colored purple and blue, respectively. The removed $Me_3Al$ is indicated by the red circle.

optimal three-coordinate O, but simultaneously lowers the coordination number of Al from four to three. However, the terminal $CH_3$ group (blue carbon in Figure 6) of another adjacent Al atom can restore four-coordination to the Al atom by bridging to this site, thus overcoming the electron deficiency created by TMA cleavage.

We next turned our attention to a possible mechanism for the oxidation process. In the experimental study,[20] addition of $Me_2AlOMe$ to MAO leads first to substitution of TMA in the precursor to anion $[\mathbf{16,6}]^-$, forming anion $[\mathbf{16,5,1}]^-$ upon subsequent addition of octamethyltrisiloxane, OMTS.[23] Over a longer time period, the precursor to the latter anion rearranges to another material which upon addition of OMTS generates the anion $[\mathbf{15,5,1}]^-$. Concomitantly, aging of both unoxidized and oxidized anion precursors occur during prolonged reaction, through net addition of MeAlO units.

In the experimental oxidation paper,[20] the MS/MS spectra of anions $[\mathbf{16,5,1}]^-$ and $[\mathbf{15,5,1}]^-$ were included as Figures S1–S4. In both cases, these anions fragment by loss of five $Me_3Al$ molecules as the collision energy is increased before they lose $Me_2AlOMe$, evidently a high energy process (see Figures S2 and S4 for breakdown graphs).[24] This is quite different from what is observed for chlorinated anions derived from MAO; in those cases loss of $Me_2AlCl$ is competitive with loss of $Me_3Al$ and occurs at lowest collision energies.[13,25]

These experimental results suggest that the initial substitution of TMA by $Me_2AlOMe$ during oxidation occurs in such a manner that the OMe group is directly incorporated into the cage versus datively bound at a type **D** site. The latter sites had been implicated in a theoretical study involving modification of **16,6** and the anion derived from it, by $Me_2AlCl$.[25]



DOI: 10.1021/acs.organomet.8b00587
*Organometallics* 2018, 37, 3936–3942

On the basis of the current theoretical results, the most likely site for this kind of substitution in **16,6** is at Site **E**. Though loss of TMA from this site is strongly endergonic, it is possible the substitution involves displacement of the bridging Al−Me−Al interaction by monomeric $Me_2AlOMe$ (present in trace amounts, hence a slow reaction) and then subsequent TMA loss (Scheme 2). Alternately, direct oxidation of the cage might be possible at this site. The substitution step is exergonic with a free energy change of −37.8 kJ mol$^{-1}$ (Table 2).

**Scheme 2. Substitution of TMA at Site E in 16,6 by $Me_2AlOMe$**

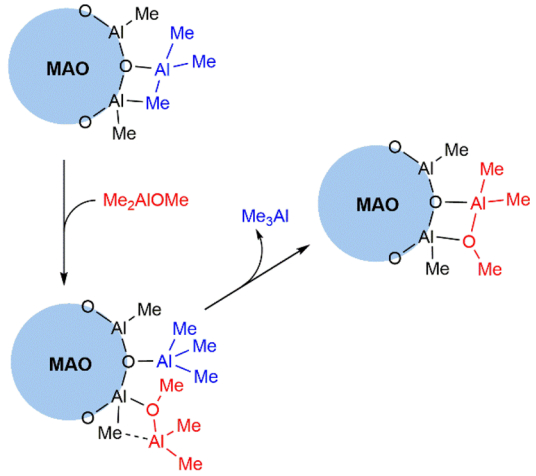


**Table 2. Energies and Gibbs Energies (kJ mol$^{-1}$) for the Proposed Oxidation Mechanism (Scheme 2)**

| entry | step | $\Delta_r E$ | $\Delta_r G^a$ |
|---|---|---|---|
| 1 | **16,6** + 1/2 $Me_4Al_2(OMe)_2$ → **16,5,1** + 1/2 $Me_6Al_2$ | −40.7 | −37.8 |
| 2 | **16,5,1** + $Me_6Al_2$ → **15,5,1** + 1/2 **2,4** | 11.7 | 36.8 |
| 3 | **16,6** + 1/2 $Me_4Al_2(OMe)_2$ + 1/2 $Me_6Al_2$ → **15,5,1** + 1/2 **2,4** | −29.0 | −1.0 |
| 4 | **16,6** + 1/2 **2,4** → **17,6** + $Me_6Al_2$ | 13.5 | −12.9 |

$^a T$ = 298 K and $p$ = 1 atm with correction to condensed phase by multiplication of the $T\Delta S$ term by 2/3.

The next step involves loss of $Me_2AlOAlMe_2$ from **16,5,1** from the site identified in Figure 7. However, direct loss of **1,1** is highly unfavorable with $\Delta G$ = 168 kJ mol$^{-1}$. Thus, we invoked binding of TMA to **16,5,1**, and loss of **1,2**, forming **15,4,1**, which then binds TMA to form **15,5,1**. However, even that process is unfavorable from a free energy perspective ($\Delta G$ = 74.2 kJ mol$^{-1}$). Therefore, as a common reference point, we assumed that the most stable form of $Me_2AlOAlMe_2$ (**2,4**) is ultimately produced following initial loss of $Me_2AlOAlMe_2$ (Table 2, entry 2). This makes the overall conversion of **16,5,1** to **15,5,1** favorable (Table 2, entry 3), but it should be borne in mind that direct loss of **2,4** is not possible from **16,5,1**.

Table 2 (entry 4) contains energies for the first step in the aging process which involves net addition of a MeAlO unit to the **16,6** cage. In the experimental studies, the aging process appeared faster during oxidation vs that of unoxidized material. This led us to propose that the byproduct of oxidation and rearrangement ($Me_2AlOAlMe_2$) was involved in the aging process. Anions and cations derived from this material have been detected in MAO using $[Bu_4N][Cl]$[13] and silicone grease[26] as additives. However, $Me_2AlOAlMe_2$ is not stable in its monomeric form, and indeed has defied structural characterization beyond the fact that it is associated in condensed phase.[27] The current calculations suggest the involvement of the most stable material formed by hydrolysis (**2,4**) in the aging process is favorable when an MeAlO unit is introduced to site **E** in **16,6**.

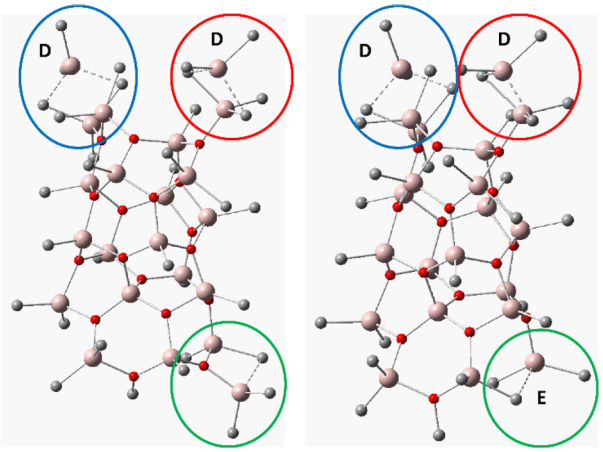


**Figure 7.** Left: **16,5,1** resulting from substitution at **E** by $Me_2AlOMe$ with a neighboring $Me_2AlOAlMe_2$ moiety circled in green. Right: **15,5,1** following loss of $Me_2AlOAlMe_2$ and binding of TMA; the newly formed type **E** site is indicated by the green circle.

Indeed, the overall steps of oxidation and aging suggest that if these processes were coupled to one another, the total free energy change is favorable (Table 2), if only the unfavorable step involving loss of $Me_2AlOAlMe_2$ can be avoided. We suspect this step is unfavorable under any circumstances since it involves cleavage of Al−O bonds. We can think of several ways in which this might be accomplished. One is the direct reaction between two cages such that a $Me_2AlOAlMe_2$ unit is exchanged between the two: **16,6** + **16,5,1** → **17,6** + **15,5,1**, $\Delta_r G$ = 23.8 kJ mol$^{-1}$

The free energy change is unfavorable (though when coupled to oxidation of **16,6**, $\Delta_r G$ = −14.0 kJ mol$^{-1}$) but certainly much less unfavorable than direct loss of $Me_2AlOAlMe_2$. We are unable to study such a process by DFT methods, but there is certainly precedent for cage−cage equilibration in MAO at elevated temperature.[14] We do note that oxidation and aging of MAO is strongly concentration-dependent as well in comparing the properties of 10−30 wt % material.[20] Another alternative that we cannot exclude is the involvement of OMTS in the (rapid) abstraction and subsequent donation of a $Me_2AlOAlMe_2$ unit from one cage to another, via a cyclic $\kappa^2$-OMTS·$\kappa^2$-$Me_2AlOAlMe_2$ moiety.

## CONCLUSION

DFT calculations at the M06-2X/TZVP level of theory have been carried out to model the oxidation of MAOs of a general formula $(MeAlO)_x(Me_3Al)_y$ up to $x$ = 18, focusing on the most stable MAOs of each degree of oligomerization located by previous computations. To evaluate the potential sites for the oxidation process, we classified the sites in to five types labeled **A**−**E**. Screening of the TMA cleavage and subsequent addition of $Me_2AlOMe$ for oxidation shows that the overall process is generally exergonic.

With specific investigations of dominant **16,6** composition, in correlation with the experimental ESI-MS studies on the corresponding anions, the calculations suggest that the initial



DOI: 10.1021/acs.organomet.8b00587
Organometallics 2018, 37, 3936−3942

substitution might occur at site **E**. Direct loss of $Me_2AlOAlMe_2$ or a related material is calculated as endergonic for all possibilities considered, so the precise mechanism for formation of **15,5,1** likely does not involve direct loss of this moiety but rather exchange of this unit with another cage or another material present in MAO. Furthermore, it could be possible that neutral **16,6** does not represent all structural features of the major anion observed in the MS experiments, though this is unlikely to affect the unfavorability of $Me_2AlOAlMe_2$ loss as this basic unit is quite unstable in monomeric form and AlO bonds must be cleaved in order to lose this fragment. Experimental and computational studies are currently ongoing to shed light on the structural differences between neutral MAOs and MAO-$Me^-$ ions.

## EXPERIMENTAL SECTION

**Computational Details.** Calculations were carried out by Gaussian 16,[28] using the meta-hybrid density functional theory M06-2X method[29] in combination with the TZVP basis set by Ahlrichs and co-workers.[30] The method has been utilized in our previous works on MAO,[16,31] and it has been shown a cost-effective method of choice for organoaluminum compounds involving dispersive interactions due to methyl groups bridging aluminums.[32] Harmonic vibrational frequencies were calculated for all reported structures to confirm them as minima in the potential energy surface and to obtain Gibbs energies ($T$ = 298 K, $p$ = 1 atm). In reporting the Gibbs energies from the gas-phase calculations, the $T\Delta S$ term of $G = H - TS$ was multiplied by 2/3 to correct for solvation entropy.[16,33,34] The uncorrected Gibbs energies are included in the Supporting Information.

## ASSOCIATED CONTENT

### Supporting Information

The Supporting Information is available free of charge on the ACS Publications website at DOI: 10.1021/acs.organomet.8b00587.

Absolute values of electronic energies, enthalpies, entropies and Gibbs energies, MS-MS spectra and break down curves of the anions [**16,5,1**] and [**15,5,1**] (PDF)

Cartesian coordinates of the reported structures (XYZ)

## AUTHOR INFORMATION


### Corresponding Author

*E-mail: mikko.linnolahti@uef.fi. Tel.: +358505926855.

### ORCID

Harmen S. Zijlstra: 0000-0002-5754-5998
Scott Collins: 0000-0001-6112-3483
J. Scott McIndoe: 0000-0001-7073-5246
Mikko Linnolahti: 0000-0003-0056-2698


### Notes

The authors declare no competing financial interest.

## ACKNOWLEDGMENTS

The computations were made possible by use of the Finnish Grid and Cloud Infrastructure resources (urn:nbn:fi:research-infras-2016072533). J.S.M. thanks NOVA Chemical's Centre for Applied Research and NSERC (Strategic Project Grant #478998-15) for operational funding and CFI, BCKDF and the University of Victoria for infrastructural support. S.C. thanks the University of Victoria for a Visiting Scientist position.

## REFERENCES


(1) Bochmann, M. The Chemistry of Catalyst Activation: The Case of Group 4 Polymerization Catalysts. *Organometallics* **2010**, *29*, 4711−4740.

(2) Zijlstra, H. S.; Harder, S. Methylalumoxane − History, Production, Properties, and Applications. *Eur. J. Inorg. Chem.* **2015**, *2015*, 19−43.

(3) Von Lacroix, K.; Heitmann, B.; Sinn, H. Behaviour of Differently Produced Methylalumoxanes in the Phase Separation with Diethyl Ether and Molecular Weight Estimations. *Macromol. Symp.* **1995**, *97*, 137−142.

(4) Babushkin, D. E.; Semikolenova, N. V.; Panchenko, V. N.; Sobolev, A. P.; Zakharov, V. A.; Talsi, E. P. Multinuclear NMR Investigation of Methylaluminoxane. *Macromol. Chem. Phys.* **1997**, *198*, 3845−3854.

(5) Hansen, E. W.; Blom, R.; Kvernberg, P. O. Diffusion of Methylaluminoxane (MAO) in Toluene Probed by $^1$H NMR Spin-Lattice Relaxation Time. *Macromol. Chem. Phys.* **2001**, *202*, 2880−2889.

(6) Babushkin, D. E.; Brintzinger, H.-H. Activation of Dimethyl Zirconocene by Methylaluminoxane (MAO) − Size Estimate for Me-MAO$^-$ Anions by Pulsed Field-Gradient NMR. *J. Am. Chem. Soc.* **2002**, *124*, 12869−12873.

(7) Stellbrink, J.; Niu, A.; Allgaier, J.; Richter, D.; Koenig, B. W.; Hartmann, R.; Coates, G. W.; Fetters, L. J. Analysis of Polymeric Methylaluminoxane (MAO) via Small Angle Neutron Scattering. *Macromolecules* **2007**, *40*, 4972−4981.

(8) Trefz, T. K.; Henderson, M. A.; Wang, M. Y.; Collins, S.; McIndoe, J. S. Mass Spectrometric Characterization of Methylaluminoxane. *Organometallics* **2013**, *32*, 3149−3152.

(9) Kilpatrick, A. F. R.; Buffet, J.-C.; Nørby, P.; Rees, N. H.; Funnell, N. P.; Sripothongnak, S.; O'Hare, D. Synthesis and Characterization of Solid Polymethylaluminoxane: A Bifunctional Activator and Support for Slurry-Phase Ethylene Polymerization. *Chem. Mater.* **2016**, *28*, 7444−7450.

(10) Zijlstra, H. S.; Linnolahti, M.; Collins, S.; McIndoe, J. S. Additive and Aging Effects on Methylalumoxane Oligomers. *Organometallics* **2017**, *36*, 1803−1809.

(11) Imhoff, D. W.; Simeral, L. S.; Sangokoya, S. A.; Peel, J. H. Characterization of Methylaluminoxanes and Determination of Trimethylaluminum Using Proton NMR. *Organometallics* **1998**, *17*, 1941−1945.

(12) Linnolahti, M.; Laine, A.; Pakkanen, T. A. Screening the Thermodynamics of Trimethylaluminum-Hydrolysis Products and Their Co-catalytic Performance in Olefin-Polymerization Catalysis. *Chem. - Eur. J.* **2013**, *19*, 7133−7142.

(13) Trefz, T. K.; Henderson, M. A.; Linnolahti, M.; Collins, S.; McIndoe, J. S. Mass Spectrometric Characterization of Methylaluminoxane-Activated Metallocene Complexes. *Chem. - Eur. J.* **2015**, *21*, 2980−2991.

(14) Falls, Z.; Tymińska, N.; Zurek, E. The Dynamic Equilibrium Between $(AlOMe)_n$ Cages and $(AlOMe)_n{\cdot}(AlMe_3)_m$ Nanotubes in Methylaluminoxane (MAO): A First-Principles Investigation. *Macromolecules* **2014**, *47*, 8556−8569.

(15) Hirvi, J. T.; Bochmann, M.; Severn, J. R.; Linnolahti, M. Formation of Octameric Methylaluminoxanes by Hydrolysis of Trimethylaluminum and the Mechanisms of Catalyst Activation in Single-Site $\alpha$-Olefin Polymerization Catalysis. *ChemPhysChem* **2014**, *15*, 2732−2742.

(16) Linnolahti, M.; Collins, S. Formation, Structure and Composition of Methylaluminoxane. *ChemPhysChem* **2017**, *18*, 3369−3374.

(17) Malpass, D. B. Commercially Available Metal Alkyls and Their Use in Polyolefin Catalysts. In *Handbook of Transition Metal Polymerization Catalysts*; Hoff, R., Mathers, R. T., Eds.; John Wiley Sons: Hoboken, NJ, 2010, 1−28.

(18) Alexandrov, Yu. A.; Vyshinskii, N. N.; Kokorev, V. N.; Alferov, V. A.; Chikinova, N. V.; Makin, G. I. On the Possibility of Complex




DOI: 10.1021/acs.organomet.8b00587
*Organometallics* 2018, 37, 3936−3942

Formation of Group IIIB Organic Compounds with Molecular Oxygen. *J. Organomet. Chem.* **1987**, *332*, 259−269.
(19) Ault, B. S. Matrix Isolation Investigation of the Reaction of $(CH_3)_3Al$ with $O_2$. *J. Organomet. Chem.* **1999**, *572*, 169−175.
(20) Zijlstra, H. S.; Collins, S.; McIndoe, J. S. Oxidation of Methylalumoxane Oligomers. *Chem. - Eur. J.* **2018**, *24*, 5506−5512.
(21) Harlan, C. J.; Bott, S. G.; Barron, A. R. Three-Coordinate Aluminum Is Not a Prerequisite for Catalytic Activity in the Zirconocene-Alumoxane Polymerization of Ethylene. *J. Am. Chem. Soc.* **1995**, *117*, 6465−6474.
(22) Atwood, J. L.; Hrncir, D. C.; Priester, R. D.; Rogers, R. D. Decomposition of High-Oxygen Content Organoaluminum Compounds. The Formation and Structure of the $[Al_7O_6Me_{16}]^-$ Anion. *Organometallics* **1983**, *2*, 985−989.
(23) Adoption of naming from ref 20 for the anions of the general formula $[(MeAlO)_x(Me_3Al)_y(Me_2AlOMe)_zMe]^- = [\boldsymbol{x,y,z}]^-$.
(24) Butcher, C. P. G.; Dyson, P. J.; Johnson, B. F. G.; Langridge-Smith, P. R. R.; McIndoe, J. S.; Whyte, C. On the use of breakdown graphs combined with energy-dependent mass spectrometry to provide a complete picture of fragmentation processes. *Rapid Commun. Mass Spectrom.* **2002**, *16*, 1595−1598.
(25) Collins, S.; Linnolahti, M.; Zamora, M. G.; Zijlstra, H. S.; Rodríguez Hernández, M. T.; Perez-Camacho, O. Activation of $Cp_2ZrX_2$ (X = Me, Cl) by Methylaluminoxane as Studied by Electrospray Ionization Mass Spectrometry: Relationship to Polymerization Catalysis. *Macromolecules* **2017**, *50*, 8871−8884.
(26) Stoddard, R. L.; Collins, S.; McIndoe, J. S. Mass spectrometry of Organoaluminum Compounds. In *The Chemistry of Organoaluminum Compounds*; Micouin, L., Marek, I., Rappoport, Z. Eds.; John Wiley & Sons, 2017; pp 77−86.
(27) Kacprzak, K.; Serwatowski, J. Organoboron water, part I: Synthesis and multinuclear magnetic resonance studies on the structure of tetramethyldialuminoxane. *Appl. Organomet. Chem.* **2004**, *18*, 394−397. and references therein.
(28) Frisch, M. J.; Trucks, G. W.; Schlegel, H. B.; Scuseria, G. E.; Robb, M. A.; Cheeseman, J. R.; Scalmani, G.; Barone, V.; Petersson, G. A.; Nakatsuji, H.; Li, X.; Caricato, M.; Marenich, A. V.; Bloino, J.; Janesko, B. G.; Gomperts, R.; Mennucci, B.; Hratchian, H. P.; Ortiz, J. V.; Izmaylov, A. F.; Sonnenberg, J. L.; Williams-Young, D.; Ding, F.; Lipparini, F.; Egidi, F.; Goings, J.; Peng, B.; Petrone, A.; Henderson, T.; Ranasinghe, D.; Zakrzewski, V. G.; Gao, J.; Rega, N.; Zheng, G.; Liang, W.; Hada, M.; Ehara, M.; Toyota, K.; Fukuda, R.; Hasegawa, J.; Ishida, M.; Nakajima, T.; Honda, Y.; Kitao, O.; Nakai, H.; Vreven, T.; Throssell, K.; Montgomery, J. A., Jr.; Peralta, J. E.; Ogliaro, F.; Bearpark, M.; Heyd, J. J.; Brothers, E. N.; Kudin, K. N.; Staroverov, V. N.; Kobayashi, R.; Normand, J.; Raghavachari, K.; Rendell, A.; Burant, J. C.; Iyengar, S. S.; Tomasi, J.; Cossi, M.; Millam, J. M.; Klene, M.; Adamo, C.; Cammi, R.; Ochterski, J. W.; Martin, R. L.; Morokuma, K.; Farkas, O.; Foresman, J. B.; Fox, D. J. *Gaussian 16*, revision B.01; Gaussian, Inc.: Wallingford CT, 2016.
(29) Zhao, Y.; Truhlar, D. G. The M06 Suite of Density Functionals for Main Group Thermochemistry, Thermochemical Kinetics, Noncovalent Interactions, Excited States, and Transition Elements: Two New Functionals and Systematic Testing of Four M06-Class Functionals and 12 Other Functionals. *Theor. Chem. Acc.* **2008**, *120*, 215−241.
(30) Schäfer, A.; Huber, C.; Ahlrichs, R. Fully Optimized Contracted Gaussian Basis Sets of Triple Zeta Valence Quality for Atoms Li to Kr. *J. Chem. Phys.* **1994**, *100*, 5829−5835.
(31) Kuklin, M. S.; Hirvi, J. T.; Bochmann, M.; Linnolahti, M. Toward Controlling the Metallocene/Methylaluminoxane-Catalyzed Olefin Polymerization Process by a Computational Approach. *Organometallics* **2015**, *34*, 3586−3597.
(32) Ehm, C.; Antinucci, G.; Budzelaar, P. H. M.; Busico, V. Catalyst Activation and the Dimerization Energy of Alkylaluminium Compounds. *J. Organomet. Chem.* **2014**, *772*−*773*, 161−171.
(33) Tobisch, S.; Ziegler, T. Catalytic Oligomerization of Ethylene to Higher Linear $\alpha$-Olefins Promoted by the Cationic Group 4 $[(\eta^5$-Cp-$(CMe_2$-bridge)-Ph)$M^{II}$(ethylene)$^2]^+$ (M = Ti, Zr, Hf) Active Catalysts: A Density Functional Investigation of the Influence of the Metal on the Catalytic Activity and Selectivity. *J. Am. Chem. Soc.* **2004**, *126*, 9059−9071.
(34) Ehm, C.; Cipullo, R.; Budzelaar, P. H. M.; Busico, V. Role(s) of TMA in Polymerization. *Dalton Trans.* **2016**, *45*, 6847−6855.


DOI: 10.1021/acs.organomet.8b00587
*Organometallics* 2018, 37, 3936−3942